PROCEEDINGS A

rspa.royalsocietypublishing.org

Research

Cite this article: Cirillo ENM, Ianiro N, Sciarra G. 2016 Compacton formation under Allen–Cahn dynamics. *Proc. R. Soc. A* **472**: 20150852.
http://dx.doi.org/10.1098/rspa.2015.0852

Received: 14 December 2015
Accepted: 11 March 2016

Subject Areas:
applied mathematics, mathematical modelling, mathematical physics

Keywords:
phase coexistence, interface, compacton, capillarity

Author for correspondence:
G. Sciarra
e-mail: giulio.sciarra@uniroma1.it

Compacton formation under Allen–Cahn dynamics

E. N. M. Cirillo[1], N. Ianiro[1] and G. Sciarra[2]

[1]Dipartimento di Scienze di Base e Applicate per l'Ingegneria, Sapienza Università di Roma, via A. Scarpa 16, Roma 00161, Italy
[2]Dipartimento di Ingegneria Chimica Materiali Ambiente, Sapienza Università di Roma, via Eudossiana 18, Roma 00184, Italy

GS, 0000-0003-1116-2980

We study the solutions of a generalized Allen–Cahn equation deduced from a Landau energy functional, endowed with a non–constant higher order stiffness. We analytically solve the stationary problem and deduce the existence of so-called compactons, namely, connections on a finite interval between the two phases. The dynamics problem is numerically solved and compacton formation is described.

1. Introduction

Phase-field models describe physical systems that can exhibit different homogeneous phases. The state of the system on the volume $\Omega \subset \mathbb{R}^3$ is coded into a so-called phase-field $u(x,t)$ depending on the space and time variables $x \in \Omega$ and $t \in [0,\infty)$, respectively. In particular, two values of the phase-field, say 0 and 1, represent the two homogeneous phases of a diphasic system. From now on we concentrate our attention on this case.

These models play a crucial role, for instance, in the study of phase reordering [1–3]: a system is quenched from the homogeneous high-temperature phase into a broken-symmetry one (a ferromagnet or a gas abruptly cooled below their critical temperature) and the evolution of the phase-field u describes the process of separation of the two phases.

A straightforward way to derive the evolution equation for the field u is that of assuming a gradient equation [4,5]

$$\frac{\partial u}{\partial t} = -\operatorname{grad} H(u) \tag{1.1}$$

associated with the Landau energy functional

$$H(u) := \int_\Omega \left[\frac{1}{2}\varepsilon \|\nabla u\|^2 + W(u)\right] \mathrm{d}x, \tag{1.2}$$

THE ROYAL SOCIETY PUBLISHING

where $W \in C^2(\mathbb{R})$ associates an energy with the phase-field u and the squared-gradient term of the phase-field variations is weighted by the energy cost ε, called *higher-order stiffness*. According to the usual physical interpretation, the energy W has to be chosen as a double well function with the two minima corresponding to the two phases 0 and 1 and $W(0) = W(1) = 0$.

If the higher-order stiffness ε is a constant positive number and no constraint to the total value of the field u is imposed, it is possible to compute the gradient of the Landau functional in the Hilbert space $L^2(\Omega)$ to get the *standard* Allen–Cahn equation

$$\frac{\partial u}{\partial t} = \varepsilon \Delta u - W'(u) \tag{1.3}$$

with normal derivative of the phase-field on the boundary equal to zero. Analogously, the Allen–Cahn equation endowed with Dirichlet or mixed boundary conditions could be derived specifying *a priori* the proper essential boundary conditions in the definition of the Hilbert space in which the gradient of the Landau functional should be computed.

The standard Allen–Cahn equation, also called the time-dependent Ginzburg–Landau equation, was introduced in [6] to describe the motion of anti-phase boundaries in crystalline solids. In this context, u represents the concentration of one of the two components of the alloy and ε is proportional to the squared interface width. A well-known explanation of this equation in terms of balance of microforces can be retrieved in [7] and the related literature. Among others one can refer to [8] for a clear statement of the continuum mechanical framework within which the Allen–Cahn (and the Cahn–Hilliard) equation(s) can be deduced.

In this paper, we consider the case in which the higher-order stiffness is not constant, but it is a sufficiently regular positive function of the field, namely, $\varepsilon \in C^2(\mathbb{R})$ such that $\varepsilon(u) \geq 0$ for any $u \in \mathbb{R}$. This situation has been considered, for instance, in [9] in which the authors studied a similar model to describe glass-like relaxation in binary fluid models. A closely connected problem, in which a not constant higher-order stiffness is used, is the study of the gas–liquid interface in capillary tubes [10]. In these cases, the gradient equation (1.1) provides the generalized Allen–Cahn equation, see appendix A,

$$\frac{\partial u}{\partial t} = \frac{1}{2}\varepsilon'(u)\|\nabla u\|^2 + \varepsilon(u)\Delta u - W'(u) \tag{1.4}$$

again with suitable conditions on the boundary $\partial\Omega$.

We focus on the one-dimensional case $\Omega = [a, b]$ and study the solutions of the Allen–Cahn equation (1.4) when the higher-order stiffness coefficient vanishes at the phases, namely, $\varepsilon(0) = \varepsilon(1) = 0$. As we shall discuss in the following section, in such a 'pathological' case there exist stationary solutions connecting the two phases on a finite interval of length $\delta > 0$. It is well known that this is not possible in the standard constant higher-order stiffness case, in which connections can only be considered on the infinite domain [11].

These solutions appeared in the scientific literature in different contexts, see, e.g. [9,10,12], and, at variance with [13], have been called *compactons*, in order to underline the property of being localized within a domain of finite measure.

Our main goal, here, is to study the behaviour of the solutions of the evolution equation (1.4) and, in particular, to describe the process leading to the formation of a compacton on the finite interval $\Omega = [a, b]$. We shall discuss both the interface Dirichlet boundary conditions

$$u(a) = 0 \quad \text{and} \quad u(b) = 1$$

and the homogeneous Neumann boundary conditions

$$u_x(a) = 0 \quad \text{and} \quad u_x(b) = 0.$$

We shall, respectively, refer to these two cases as the (D)- and (N)-boundary conditions.

Let us summarize our main result. Compactons can be used to construct stationary solutions of the Allen–Cahn equation performing many excursions between the two phases, whose total number is bounded by $(b - a)/\delta$. In the standard Allen–Cahn stationary problem, i.e. when the

higher-order stiffness coefficient is constant, stationary profiles oscillating between the two phases are not allowed when (D)-boundary conditions are imposed. On the other hand, it is possible to construct profiles oscillating between two values of the phase-field u 'close' to the two pure phase values in the (N)-boundary condition case. These solutions, in the conservative mechanics equivalent model language in which the stationary Allen–Cahn model can be immediately recasted, correspond to the periodic motions of the system with total (kinetic plus potential) energy slightly smaller than zero.

In the (N)-boundary condition case single interface and periodic profiles are proved to be unstable [14,15].

We then expect that any time-dependent solution of the Allen–Cahn evolution equation, for any choice of the initial profile, will never tend in the long time limit to one of these oscillating stationary solutions. In other words, the standard Allen–Cahn evolution cannot create an alternating profile and, indeed, such an equation is used to model domain coarse-graining in phase separation.

The question we pose in this paper is the following: in the presence of compactons, can the Allen–Cahn evolution describe the alternating profile formation? In this paper, by means of a numerical computation in the framework of a specific model, we shall give a positive answer to such a question. In particular, we shall show that the alternating compacton profile formation is possible with both (D)- and (N)-boundary conditions.

In our study, we shall use the following techniques: the stationary solution of the Allen–Cahn equation (1.4) will be studied analytically and the 'usual' qualitative Weierstrass study will allow the construction of the phase portrait which will provide a thorough description of the structure of the stationary profiles. On the other hand, the time-dependent solutions will be studied numerically and a code based on the finite-element method will be adopted.

In order to perform the numerical study a particular choice of the functions $\varepsilon(u)$ and $W(u)$ will be done. We borrow those functions from [10] where a model describing the gas–liquid interface in a capillary tube has been proposed. It is worth noting that we shall not discuss the evolution equations proposed in [10], but the Allen–Cahn equation with stationary profiles coinciding with the ones in the [10] model. Indeed, our main interest is that of understanding the Allen–Cahn evolution in the presence of compactons and to this aim we have chosen, as a prototype model, the one in [10] whose stationary solutions has a clear physical interpretation. Moreover, this model allows us to study analytically the compactons, whose behaviour can be expressed in terms of special functions. This will provide us with an effective analytical control of our numerical results.

One of the main results in [10] is the possibility to describe the existence of local, non-spreading and compactly supported bubbles in a capillary tube. In that paper, the model was studied numerically. Here we solve analytically the equation giving the stationary states of the system and explain some of the features of the compacton solutions presented in [10].

The paper is organized as follows: in §2, we discuss under quite general hypotheses the existence of compactons for the stationary Allen–Cahn equations. In §3, we consider the model introduced in [10] to study the gas–liquid interface in capillary tube and, in such a context, we find explicitly (in terms of special function) the compacton solutions and discuss their main physical properties. In §4, we study numerically the solutions of the Allen–Cahn equation with higher-order stiffness ε and energy W as in [10]. Section 5 is devoted to some brief conclusions.

2. Compactons

We consider the Allen–Cahn problem (1.4) on the one-dimensional space $[a, b]$. The equation for the stationary solutions $u = u(x)$ then becomes

$$\varepsilon(u)u_{xx} + \tfrac{1}{2}\varepsilon'(u)u_x^2 - W'(u) = 0. \tag{2.1}$$

Here, and in the following, the prime will always denote the derivative with respect to the natural argument, whereas space (time) derivatives will be written explicitly as $\mathrm{d}/\mathrm{d}x$ or with a subscript x ($\mathrm{d}/\mathrm{d}t$ or with a subscript t).

We assume $W(u) = W_0 u^2(1-u)^2$, with $W_0 > 0$, and $\varepsilon \in C^2([0,1])$ such that $\varepsilon(u) > 0$ for $u \in (0,1)$, and $\varepsilon(0) = \varepsilon(1) = 0$. The choice of the potential energy W with two isoenergetic minima models the existence of two coexisting phases. Moreover, we assume that ε tends to 0 in 0 and 1 at least as a power law, namely, there exists $\chi > 0$ such that

$$\lim_{u\to 0^+} \frac{\varepsilon(u)}{u^\chi} = 0 \quad \text{and} \quad \lim_{u\to 1^-} \frac{\varepsilon(u)}{(1-u)^\chi} = 0.$$

The two last assumptions are crucial for the compacton existence,[1] see (2.3) and the discussion which follows, as well as the related arguments in [9,10].

It is very important to remark that any regular solution $u(x)$ of (2.1) is such that the conservation law

$$\frac{\mathrm{d}}{\mathrm{d}x}\left[\frac{1}{2}\varepsilon(u)u_x^2 - W(u)\right] = 0 \tag{2.2}$$

is satisfied.

Note that the problem is similar, see also [16–19], to that of an holonomic conservative mechanical system with Lagrangian coordinate u, not constant mass matrix $\varepsilon(u)$, and potential energy of the conservative force $-W(u)$, once the space variable x is interpreted as time. A lot of care has to be used when one wants to exploit this analogy, as the mass matrix $\varepsilon(u)$ is not positive defined, but it is equal to zero in the pure phases $u = 0$ and $u = 1$.

The aim of this model is that of describing a compact interface (or connection) between the pure phases $u = 0$ and $u = 1$, namely, we look for a solution of (2.1) equal to zero on a finite (say left) space interval, equal to one on a finite (say right) space interval, and continuously joining these two pure phases on an intermediate 'finite' space interval. This intermediate interval will be the compact interface (or connection) between the two pure phases.

In standard cases, i.e. when the higher-order stiffness coefficient is constant, an interface with zero derivative at the boundary can only be achieved on the whole $\mathbb{R}$ (heteroclinic problem). This property is very general and is connected to the uniqueness of the solution of a Cauchy problem which is ensured if the differential equation describing the interface is sufficiently regular. In the model we are studying here, this regularity of the equation is not satisfied due to the presence of the not positive definite mass matrix $\varepsilon(u)$. This is the key peculiarity of the model that gives rise to the existence of compacton solutions.

First of all, we note that the constant functions $u(x) = 0$ and $u(x) = 1$ trivially satisfy (2.1). So that we can imagine to construct a solution of this equation such that $u(x) = 0$ for all $x \in [a, c]$ and $u(x) = 1$ for all $x \in [c + \delta, b]$, with $c, \delta \in \mathbb{R}$ given. The problem, now, is that of finding the interface joining the two pure phases on the 'finite' interval $[c, c + \delta]$. Note that the pure phases fix the value of the constant of motion (2.2) to zero; hence, the interface we are looking for has to satisfy

$$\tfrac{1}{2}\varepsilon(u(x))u_x^2 - W(u(x)) = 0 \quad \text{for } x \in [c, c+\delta].$$

By separation of variables we get the implicit solution

$$x - c = \int_0^u \sqrt{\frac{\varepsilon(y)}{2W(y)}}\,\mathrm{d}y. \tag{2.3}$$

As we assumed ε to vanish in 0 and 1 at least as a power, we have that the integral above is convergent on the interval $[0, 1]$. Hence, we have proved the existence of the compacton and we can also conclude that

$$\delta = \int_0^1 \sqrt{\frac{\varepsilon(u)}{2W(u)}}\,\mathrm{d}u \tag{2.4}$$

expresses its width.

[1] We have chosen the Duffing potential energy W for simplicity. The same discussion can be repeated for very general double well potential energies, but the condition on the higher-order stiffness coefficient have to be chosen accordingly.

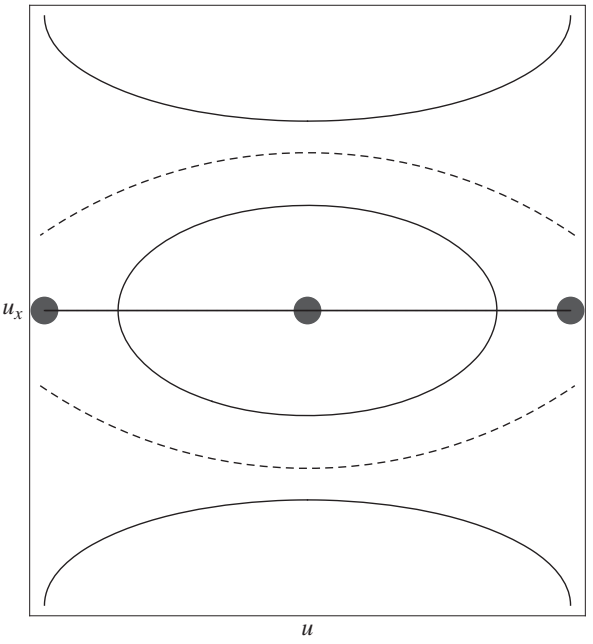

Figure 1. A possible phase portrait of the stationary equation (2.1). The dotted lines represent the compactons: in the picture they assume finite values at $u = 0$ and $u = 1$, but, recall, they could also tend to zero or diverge (see also figure 2).

We close this section by noting that, by means of the conservation law, it is possible to describe the structure of all the solutions of the stationary equation (2.1). Indeed, (2.2) ensures that any regular solution satisfies the equation

$$\tfrac{1}{2}\varepsilon(u)u_x^2 - W(u) = E \tag{2.5}$$

for some $E \in \mathbb{R}$.

The structure of the solution of the equation (2.5) lying in the interval $0 \le u \le 1$ is as follows. For $E = 0$ the constant, $u(x) = 0$ and $u(x) = 1$, solutions and combination of them with compactons are found. Note that, as we assumed a power law behaviour of $\varepsilon(u)$ for $u \to 0, 1$, we have that the space derivative of the profile can be zero, finite or divergent in the phases 0 and 1. For $E > 0$, as $\varepsilon(u)$ vanishes in $u = 0$ and $u = 1$, the profile $u(x)$ must have divergent derivative in 0 and 1. For $-W_0/16 < E < 0$, the solution is bounded to the region in which $W(u) + E \ge 0$; as in such a region $\varepsilon(u) > 0$, we find a classical oscillating solution. Finally, for $E = -W_0/16$, the unique solution is the constant $u(x) = \frac{1}{2}$.

These results are summarized in figure 1 in which the three points represent the constant solutions $u(x) = 0$, $u(x) = \frac{1}{2}$ and $u(x) = 1$, the dotted lines represent the compactons, the lines diverging in 0 and 1 are the solutions for $E > 0$, and, finally, the closed loops are the solutions for $-W_0/16 < E < 0$. Note that in the figure we have depicted the compacton line finite at the phases, but, as we discussed above, it can happen that close to the phases the line tends to zero or diverges.

Recalling that δ denotes the length of the compactons solution, note that the length

$$\delta_{\mathrm{u}}(E) = \int_0^1 \sqrt{\frac{\varepsilon(y)}{2[E + W(y)]}}\,\mathrm{d}y$$

of profiles connecting the two phases 0 and 1 and corresponding to $E > 0$ is such that

$$\delta_{\mathrm{u}}(E) < \delta \quad \text{for } E > 0.$$

On the other hand, for $E<0$, we let $0<u_-(E)<u_+(E)<1$ be the two solutions of the equation $W(u)+E=0$ lying in the open interval $(0,1)$. Hence, the length of a single interface connecting $u_-(E)$ to $u_+(E)$ is given by

$$\delta_{\mathrm{d}}(E)=\int_{u_-(E)}^{u_+(E)}\sqrt{\frac{\varepsilon(y)}{2[E+W(y)]}}\,\mathrm{d}y.$$

This analysis on the phase space trajectories allows us to state the following results about the existence of solutions of the stationary problem. The stationary equation (2.1) with (D)-boundary conditions has a unique solution corresponding to a phase line with $E>0$ if $b-a<\delta$, has the unique compacton solution if $b-a=\delta$, and has infinite solutions if $b-a>\delta$ which can be constructed by gluing compactons and pure phase constant segments.

The stationary equation (2.1) with (N)-boundary conditions has always the two pure phase constant solutions $u(x)=0$ and $u(x)=1$. If $b-a$ is large enough, so that for some $E<0$ one has $\delta_{\mathrm{d}}(E)<b-a$, the problem can have single connection or oscillating solutions connecting two points $0<u_-<u_+<1$ and corresponding to the phase lines with $E<0$. Moreover, if $b-a>\delta$ the problem has also solutions which can be constructed by gluing compactons and pure phase constant segments.

3. Bubbles in a capillary tube

A one-dimensional model is adopted for describing the spatial distribution, in a capillary tube, of the liquid and the gaseous phases regarding the mixture as a non-uniform fluid, which means, according to [20], a system having a spatial variation of one of its intensive scalar properties. In particular, following [10] one can assume this property, say the phase-field u introduced in §2, to be the density of the gas with respect to the volume locally available. In the specific case of a capillary tube with a constant section, the phase-field is the fraction of the cross-sectional area of the tube occupied by the gaseous phase S_{g}, per unit length of the tube.

Apparently, the gas saturation S_{g} can be related to the volume density of the liquid phase S_{l} keeping in mind the obvious constraint

$$S_{\mathrm{g}}+S_{\mathrm{l}}=1. \tag{3.1}$$

According to the general formulation presented in §2, a Landau energy functional is introduced whose density per unit volume is the sum of a bulk contribution, prescribed in terms of a double well potential, $F(S_{\mathrm{g}})$, and an energy penalty for gradients of the gas saturation S_{g}, affected by the current value of S_{g}. In order to characterize the admissible equilibrium configurations of the system, we refer from now on to the constitutive model given in [10]. Assuming the equilibrium between the gaseous and the liquid phase to be controlled only by capillary forces and, therefore, by the adjustment of the contact angle $\theta\in(0,\pi)$ between the gas–liquid and the liquid–solid interfaces, see [21], the double well potential $F(S_{\mathrm{g}})$ is prescribed following [10] by

$$F(S_{\mathrm{g}})=\frac{\gamma(1-\cos\theta)}{R}(1-S_{\mathrm{g}})^2S_{\mathrm{g}}^2+\frac{\gamma\cos\theta}{R}[(1-S_{\mathrm{g}})^2-S_{\mathrm{g}}^2], \tag{3.2}$$

γ being the surface energy relative to the gas–liquid interface, and R the radius of the capillary tube. Following [10] the higher-order stiffness will be written in terms of the product of

$$\Gamma=C_\Gamma\gamma R(1-\cos\theta)\left[\frac{1-\sin\theta}{\cos\theta}\right]^2 \tag{3.3}$$

and

$$k(S_{\mathrm{g}})=S_{\mathrm{g}}^{\alpha}(1-S_{\mathrm{g}})^{\beta}, \tag{3.4}$$

with $\alpha=2-\cos\theta$, $\beta=2+\cos\theta$. In [10], a dimension argument is given for the definition of Γ, moreover, it is remarked that the peculiar expression of k plays a key role in the existence of compact interfaces, see also [9].

The derivative of the double well potential (3.2) specifies the difference between the chemical potential of the gas and the chemical potential of the liquid or, analogously, the negative chemical potential μ of the liquid, once that of the gas has been fixed to zero, as a reference value. Its value at the pure phases, $S_g = 1$, the gas, and $S_g = 0$, the liquid, is the same, say

$$\left.\frac{\partial F}{\partial S_g}\right|_{S_g=0} = \left.\frac{\partial F}{\partial S_g}\right|_{S_g=1} = -2\frac{\gamma\cos\theta}{R}, \tag{3.5}$$

so that, according with classical Maxwell's rule, the non-uniform fluid exhibits coexistence of the two phases at equilibrium only when the chemical potential is uniformly equal to $\mu = \partial F/\partial S_g = -2\gamma\cos\theta/R$ over the whole spatial domain. Requiring this condition to be verified corresponds to find out the solutions of the minimization problem

$$\min_{S_g}\left(F(S_g) + 2\frac{\gamma\cos\theta}{R}S_g\right), \tag{3.6}$$

which admits two solutions at $S_g = 0$ and $S_g = 1$. Owing to the additional linear term, $2\gamma\cos\theta/RS_g$ the two phases correspond, now, to two isopotential minima of the function $F(S_g) + 2\gamma\cos\theta/RS_g$.

The regularization provided by the energy penalty proportional to the squared-gradient term via the higher-order stiffness $\Gamma k(S_g)$, see equations (3.3)–(3.4), implies, at coexistence, the conservation law (2.2) to be rewritten as follows:

$$0 = \frac{2\gamma}{R}(1-\cos\theta)(1-S_g)S_g(1-2S_g) - \Gamma\sqrt{k(S_g)}\frac{\mathrm{d}}{\mathrm{d}x}\left(\sqrt{k(S_g)}\frac{\mathrm{d}}{\mathrm{d}x}S_g\right), \tag{3.7}$$

which therefore reads as a specialization of the Allen–Cahn equation when a non-uniform fluid is placed into a capillary tube.

(a) The compact interface problem

From now on, we shall simplify the notation by letting $S_g = S$ and rewrite equation (3.7) as

$$\Gamma k(S)S_{xx} + \tfrac{1}{2}\Gamma S_x^2 k'(S) - V'(S) = 0, \tag{3.8}$$

where we have set

$$V(S) = F(S) + 2S\frac{\gamma}{R}\cos\theta - \frac{\gamma}{R}\cos\theta = \frac{\gamma}{R}(1-\cos\theta)(1-S)^2S^2. \tag{3.9}$$

In order for the physical dimensions of the quantities introduced above to be consistent with the notation of §1 a suitable viscosity parameter μ must be introduced so that $W = F/\mu$ and $\varepsilon = \Gamma k(S)/\mu$.

It is important to remark that the interface problem (3.8) in the capillarity set-up is an example of applications of the theory developed in §2. Thus, as discussed in §2, in order to ensure that the integral (2.3) is convergent, it is sufficient to require that the parameters α, β in (3.4) are strictly positive. In other words, the particular dependence of α and β on the contact angle θ discussed below (3.4) is not necessary to prove the existence of compactons, but, as we shall see below, affects their width δ. Indeed, by (2.4) we get

$$\delta = \int_0^1 \frac{y^{-(1/4)\cos\theta}(1-y)^{(1/4)\cos\theta}}{\sqrt{2\gamma(1-\cos\theta)/(R\Gamma)}}\,\mathrm{d}y, \tag{3.10}$$

for the compacton width. Moreover, by (B 9), we have

$$\delta = \frac{1}{\sqrt{2\gamma(1-\cos\theta)/(R\Gamma)}}\frac{(\pi/4)\cos\theta}{\sin[(\pi/4)\cos\theta]}.$$

Finally, recalling (3.3), we get

$$\delta = R\sqrt{\frac{C_\Gamma}{2}}\frac{1-\sin\theta}{|\cos\theta|}\frac{(\pi/4)\cos\theta}{\sin[(\pi/4)\cos\theta]}. \tag{3.11}$$

(b) Compacton profile

As above it is possible to write an implicit expression of the compacton profile $S(x)$ in terms of special functions. Indeed, by performing the same computation as above, from (2.3) we get

$$x(S) - c = \int_0^S \frac{y^{-(1/4)\cos\theta}(1-y)^{(1/4)\cos\theta}}{\sqrt{2\gamma(1-\cos\theta)/(R\Gamma)}}\,\mathrm{d}y. \tag{3.12}$$

Equation (B 8) and some simple algebra yields

$$x(S) - c = R\sqrt{\frac{C_\Gamma}{2}}\frac{1-\sin\theta}{|\cos\theta|}B\left(S, 1-\frac{1}{4}\cos\theta, 1+\frac{1}{4}\cos\theta\right), \tag{3.13}$$

where we have denoted by B the incomplete beta function, see (B 2) in appendix B, which gives implicitly the profile of the compacton $S(x)$ for $x \in (c, c+\delta)$.

By using the explicit solution given above, many interesting physics features of the compactons discussed in [10] can be proved analytically. For instance, in that paper it has been noted that the convexity of the interface profile $S(x)$ for $x \in [c, c+\delta]$ depends on whether the liquid phase has a wetting ($\theta > \pi/2$, for instance water) or a not wetting ($\theta < \pi/2$, for instance mercury) behaviour. By means of (3.13), this problem is reduced to a simple computation. Indeed, recall that the compacton satisfies (3.8) and along the compacton the constant of motion (2.2) is equal to zero; thus, from (3.8) and (2.2), we get that

$$\Gamma k(S)S_{xx} = V(S)\left[\frac{1}{V(S)}V'(S) - \frac{1}{k(S)}k'(S)\right],$$

for any $x \in (c, c+\delta)$. A simple computation yields

$$\frac{1}{V(S)}V'(S) = \frac{2(1-2S)}{S(1-S)} \quad \text{and} \quad \frac{1}{k(S)}k'(S) = \frac{\alpha - 4S}{S(1-S)}.$$

Thus, for any $x \in (c, c+\delta)$, we have that

$$S_{xx}(x) = \frac{V(S(x))}{2\Gamma S(x)[1-S(x)]k(S(x))}\cos\theta. \tag{3.14}$$

As $\Gamma \geq 0$, and $V(S(x))$, $S(x)$, $1-S(x)$ and $k(S(x))$ are strictly positive in the open interval $(c, c+\delta)$, we have that the profile is convex for $\theta < \pi/2$ (not wetting liquid) and not convex for $\theta > \pi/2$ (wetting liquid).

(c) Phase portrait

In this section, we discuss the structure of the solutions of the stationary equation (3.8) by means of the qualitative Weierstrass analysis. The conservation law (2.2) in this case reads

$$\tfrac{1}{2}\Gamma k(S)S_x^2 - V(S) = E, \tag{3.15}$$

with $E \in \mathbb{R}$.

The phase portrait of the model can be deduced by solving (3.15) with respect to S_x. Following [10], we assume $C_\Gamma = \frac{3}{2}$, while the other parameters are chosen to simplify the numerical calculation as $\gamma = 1$, $R = 1$ and $\theta = \pi/4$. With these assumptions, we find the drawing depicted in figure 2. The discs in the pictures denote the constant solutions, the line tending to zero in zero represents the compacton, closed curves are associated with the cases $E < 0$, the remaining lines represent the profiles in the case $E > 0$.

In order to find the stationary profiles one has to integrate the equation (3.15). For $E = 0$, the solutions of (3.15) are the constant profiles $S(x) = 0$ and $S(x) = 1$, and the compacton. For $E > 0$, the problem of finding the stationary profiles (in an implicit form) is reduced to the computation

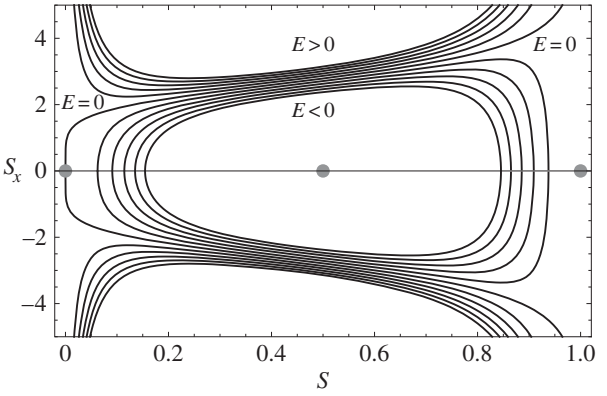

Figure 2. Phase portrait associated with the equation (3.15) for $\gamma = 1, R = 1, C_\Gamma = \frac{3}{2}$ and $\theta = \pi/4$.

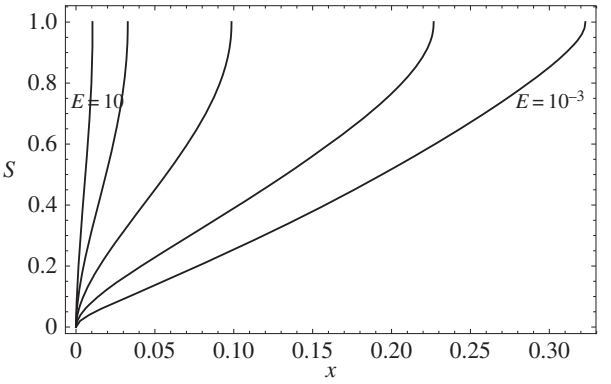

Figure 3. From the left to the right, we plot the stationary profiles of the equation (3.8) computed via the integral (3.16) for $E = 10, 1, 0.1, 0.01, 0.001$. Parameters: $\gamma = 1, R = 1, C_\Gamma = \frac{3}{2}$ and $\theta = \pi/4$.

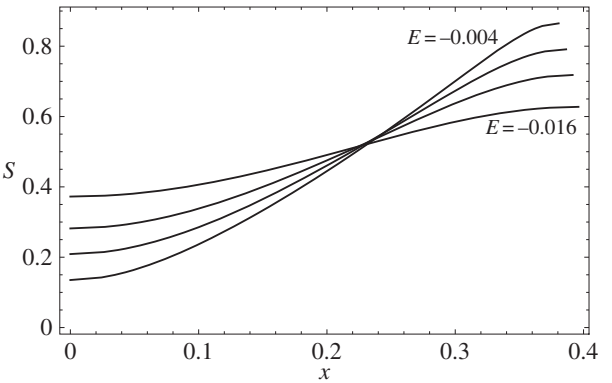

Figure 4. We plot the stationary profiles of the equation (3.8) computed via the integral (3.17) for $E = -0.016, -0.012, -0.008, -0.004$. Parameters: $\gamma = 1, R = 1, C_\Gamma = \frac{3}{2}$ and $\theta = \pi/4$.

of the definite integral (figure 3)

$$x = \int_0^{S(x)} \sqrt{\frac{\Gamma k(y)}{2[E + V(y)]}}\, \mathrm{d}y. \tag{3.16}$$

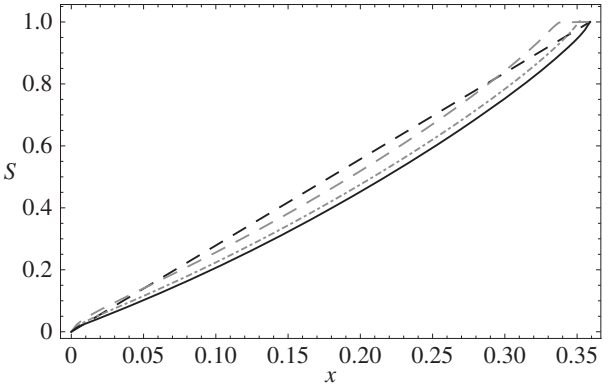

Figure 5. Allen–Cahn dynamics with (D)-boundary conditions and a linear initial profile (dashed black) connecting the two phases. Two intermediate profiles (dashed grey) and the stationary profile (solid black) are depicted. The domain of length $(b-a)=19/20\delta$ is discretized into 10^2 finite elements, the time needed to get a distance of 10^{-3} between two subsequent profiles is $t_f=189$.

For $E<0$, denoted by $S_-<S_+$ the two solutions of the equation $V(S)+E=0$, lying in the open interval $(0,1)$, which rephrases the condition of vanishing derivative of S, the problem of finding the stationary profiles (in an implicit form) is reduced to the computation of the definite integral (figure 4)

$$x=\int_{S_-}^{S(x)}\sqrt{\frac{\Gamma k(y)}{2[E+V(y)]}}\,\mathrm{d}y. \tag{3.17}$$

4. Approaching compactons

Once defined the admissible stationary configurations, which solve (2.5), in particular those describing the spatial distribution of the liquid and the gaseous phases in a capillary tube, see (3.13), (3.16) and (3.17) and figures 3 and 4, it is interesting to discuss which of them can be attained through the dissipative evolution described by the Allen–Cahn equation (1.4), endowed with (D)- or (N)-boundary conditions.

In the following, the solutions of the Allen–Cahn equation with (D)- and (N)-boundary conditions are separately discussed when considering $(b-a)<\delta$, say the length of the interval smaller than the length of the compacton, and $(b-a)>\delta$. In the first case, no compacton stationary profile is admissible, conversely in the second one, suitable profiles, constructed gluing compactons and pure phases, are admissible solutions of the problem. The time-dependent spatial profiles are numerically captured using a finite-element code which has been implemented within MATHEMATICA. Time is made dimensionless with respect to the ratio $\mu/(\gamma/R)$.

Let $(b-a)<\delta$. In this case, the dynamics does not tend to the compacton simply because there is not sufficient space for the compacton to arise. Assuming (D)-boundary conditions, the stationary configuration is a regular profile (figure 5), whereas for (N)-boundary conditions the dynamics tends to one of the two pure phases, depending on the initial data (figure 6). It is interesting to note that intermediate profiles of S, for (D)-boundary conditions, can be obtained gluing regular profiles, of length smaller than $(b-a)$, similar to those of figure 3, and pure phase solutions (in particular, $S=1$), where the measure of the subdomain corresponding to this last partial solution fades away with increasing time. On the other hand, assuming (N)-boundary conditions, the evolution passes through a progressive flattening of the profiles.

Consider now $(b-a)>\delta$, for both (D)- and (N)-boundary conditions, two different situations are discussed corresponding to a length of the interval $(b-a)$ larger or much larger than δ. In the first case only one compacton can arise whereas in the second one more than one compacton

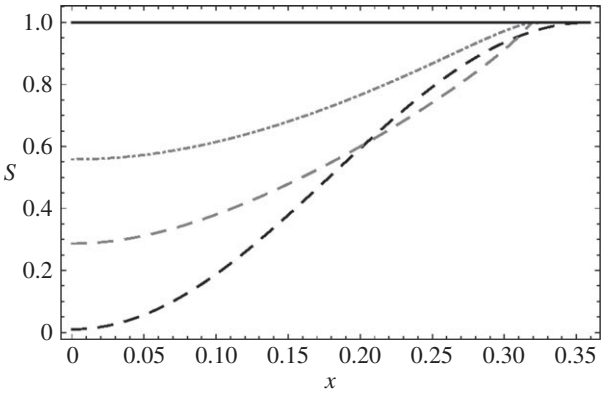

Figure 6. Allen–Cahn dynamics with (N)-boundary conditions and a branch of a sinusoidal-type initial profile (dashed black) connecting the two phases. Two intermediate profiles (dashed grey) and the stationary profile (solid black) are depicted. The domain of length $(b - a) = 19/20\delta$ is discretized into 10^2 finite elements, the time needed to get a distance of 10^{-3} between two subsequent profiles is $t_f = 39$.

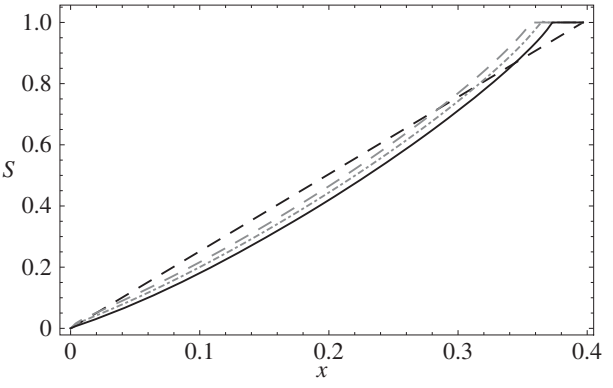

Figure 7. Allen–Cahn dynamics with (D)- and (N)-boundary conditions and a linear initial profile (dashed black) connecting the two phases. Two intermediate profiles (dashed grey) and the stationary profile (solid black) are depicted. The domain of length $(b - a) = 21/20\delta$ is discretized into 10^2 finite elements; after 500 dimensionless time steps, with $\Delta t = 2$. The distance between two subsequent profiles was $d^{(D)} = 0.00013765$ and $d^{(N)} = 0.000108560687$ for the two cases.

can form, depending on the initial conditions. Assume a linear initial profile connecting the two phases and the length of the interval close to the length of the compacton, for instance $(b - a) = 21/20\delta$; the dynamics is definitely similar to that in figures 5 and 6, where the stationary profile is indeed formed by the compacton and the solution corresponding to the pure phase $S = 1$ (figure 7).

Consider now an interval whose length is $(b - a) = 6\delta$. In this case, depending on the initial conditions, one or more compactons can form in the domain so that oscillating solutions can indeed correspond to stationary states of the Allen–Cahn dissipative dynamics. In figures 8 and 9, two distinct cases are exhibited which correspond to (D)- and (N)-boundary conditions. In particular, in figure 8, a non-oscillating and an oscillating profile are obtained starting from different initial data.

5. Conclusion

We have considered a generalized Allen–Cahn equation deduced from a Landau energy functional with a non-constant higher-order stiffness vanishing at the two pure phases. We have

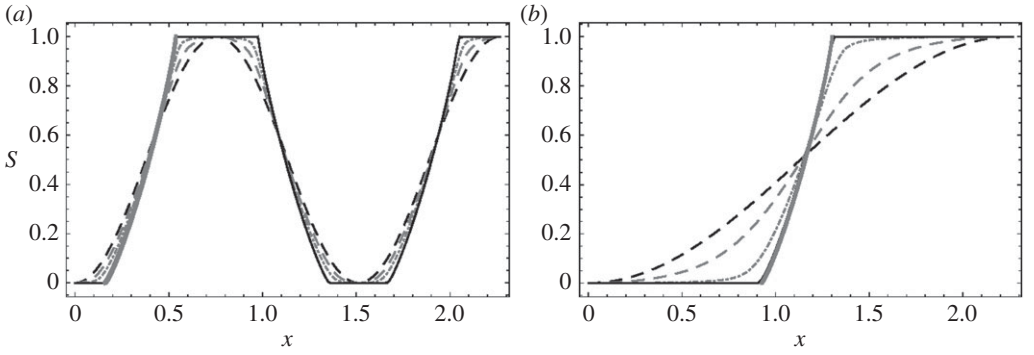

Figure 8. Allen–Cahn dynamics with (D)-boundary conditions and two co-sinusoidal initial profiles (dashed black), connecting the two phases; the initial data are periodic of period 4δ and 12δ, respectively, in the left and the right panel. Two intermediate profiles (dashed grey), the stationary profiles (solid black) and the compacton profiles (thick solid grey) are depicted. The domain of length $(b - a) = 6\delta$ is discretized into 2×10^2 finite elements; the time needed to get a distance of 10^{-3} between two subsequent profiles is $t_f = 29$ and $t_f = 25$, respectively.

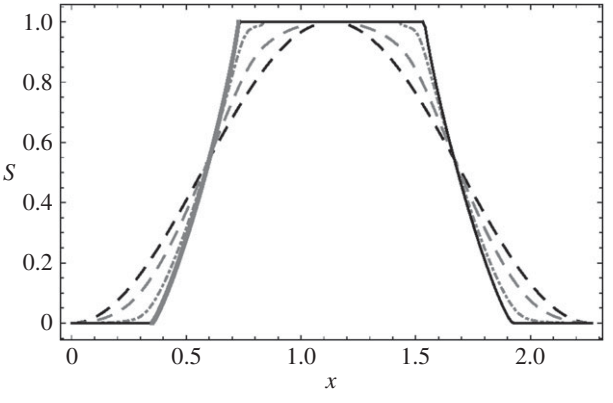

Figure 9. Allen–Cahn dynamics with (N)-boundary conditions and a co-sinusoidal type initial profile (dashed black) connecting the two phases. Two intermediate profiles (dashed grey), the stationary profile (solid black) and the compacton profile (thick solid grey) are depicted. The domain of length $(b - a) = 6\delta$ is discretized into 2×10^2 finite elements; the time needed to get a distance of 10^{-3} between two subsequent profiles is $t_f = 35$.

solved analytically the stationary problem and deduced the existence of the so-called compactons. We have also shown the possibilities of piecewise stationary solutions made of the superposition of compactons and constant pure phase profiles.

In a case of particular physical interest, the compacton problem has been solved explicitly and the main physical features of such profiles connecting a liquid and a gas phase in a capillarity tube have been deduced.

The dynamics has been studied numerically and the compacton formation has been described in detail. In this framework, one of the most relevant result we discussed is the possibility that, due to the presence of compactons and by choosing the initial condition properly, the dissipative Allen–Cahn evolution can result in the formation of periodic profiles connecting the two pure phases. This stationary profiles pops up as the long time limit of the dynamical problem. It is important to stress that this possibility is ruled out in the standard Allen–Cahn dynamics.

Data accessibility. The work does not include any experimental data. All computational results presented in the examples of the paper are reproducible using the analytical methods detailed in the article and the appendices. All numerical computations were performed in MATHEMATICA.

Authors' contributions. All the authors have provided substantial contributions to the conception and design of the model, analysis and interpretation of the results, writing the article and revising it following the comments and suggestions of the anonymous referees. All authors have given their final approval of the version to be published.

Competing interests. The authors of the paper have no competing interests.

Funding. No source of funding.

Acknowledgements. We wish to express our thanks to P. Buttà for very useful discussions.

Appendix A. Derivation of the Allen–Cahn equation

For completeness, we sketch the derivation of the Allen–Cahn equation (1.4) in the case in which the higher-order stiffness coefficient is not constant.

The gradient $\operatorname{grad} H$ of the Landau functional (1.2) in the space $L^2(\Omega)$ is a function in such a space such that

$$\frac{\mathrm{d}}{\mathrm{d}s}H(u+sv)\Big|_{s=0} = \int_\Omega v \operatorname{grad} H \,\mathrm{d}x,$$

for any $v \in L^2(\Omega)$. In other words, the derivative of the function in any direction is equal to the scalar product of such a function with the one characterizing the direction. By (1.2), it follows that

$$\frac{\mathrm{d}}{\mathrm{d}s}H(u+sv) = \int_\Omega \left[\frac{1}{2}\varepsilon'(u+sv)\|\nabla u + s\nabla v\|^2 v + \varepsilon(u+sv)(\nabla u + s\nabla v)\cdot\nabla v + W'(u+sv)v\right]\mathrm{d}x$$

and hence

$$\frac{\mathrm{d}}{\mathrm{d}s}H(u+sv)\Big|_{s=0} = \int_\Omega \left[\frac{1}{2}\varepsilon'(u)\|\nabla u\|^2 v + \varepsilon(u)\nabla u\cdot\nabla v + W'(u)v\right]\mathrm{d}x.$$

For $f, g, h : \mathbb{R}^3 \to \mathbb{R}$ sufficiently regular, we recall the Green identity

$$\int_\Omega f\nabla g\cdot\nabla h\,\mathrm{d}x = -\int_\Omega h\nabla\cdot(f\nabla g)\,\mathrm{d}x + \int_{\partial\Omega} hf\frac{\partial g}{\partial n}\,\mathrm{d}S$$

with $\partial\Omega$ the boundary of Ω and $\partial g/\partial n$ the derivative in the direction orthogonal to the boundary. We then get

$$\frac{\mathrm{d}}{\mathrm{d}s}H(u+sv)\Big|_{s=0} = \int_\Omega \left[\frac{1}{2}\varepsilon'(u)\|\nabla u\|^2 - \nabla\cdot(\varepsilon(u)\nabla u) + W'(u)\right]v\,\mathrm{d}x + \int_{\partial\Omega} v\varepsilon(u)\frac{\partial u}{\partial n}\,\mathrm{d}S.$$

Moreover, recalling the properties of the divergence operator we get

$$\frac{\mathrm{d}}{\mathrm{d}s}H(u+sv)\Big|_{s=0} = \int_\Omega \left[-\frac{1}{2}\varepsilon'(u)\|\nabla u\|^2 - \varepsilon(u)\Delta u + W'(u)\right]v\,\mathrm{d}x + \int_{\partial\Omega} v\varepsilon(u)\frac{\partial u}{\partial n}\,\mathrm{d}S.$$

Finally, from this equality, in the Lebesgue space of functions such that the normal derivative to the boundary of Ω vanishes, we have that

$$\operatorname{grad} H(u) = -\tfrac{1}{2}\varepsilon'(u)\|\nabla u\|^2 - \varepsilon(u)\Delta u + W'(u),$$

which yields the Allen–Cahn equation (1.4).

Appendix B. Integral computations

The integrals (3.10) and (3.12) can be computed by using the properties of the gamma and beta functions.

Recall the definition of the beta function and that of the incomplete beta function

$$B(p,q)=\int_0^1 t^{p-1}(1-t)^{q-1}\,\mathrm{d}t \tag{B 1}$$

and

$$B(x,p,q)=\int_0^x t^{p-1}(1-t)^{q-1}\,\mathrm{d}t \tag{B 2}$$

with $\mathrm{Re}(p),\mathrm{Re}(q)>0$. It is immediate to prove that

$$B(p,q)=B(1,p,q) \tag{B 3}$$

and

$$\frac{\mathrm{d}}{\mathrm{d}x}[xB(x,p,q)-B(x,p+1,q)]=B(x,p,q). \tag{B 4}$$

In the following, we shall also need some properties of the gamma function. Recall its definition

$$\Gamma(p)=\int_0^\infty t^{p-1}\mathrm{e}^{-t}\,\mathrm{d}t \tag{B 5}$$

with $\mathrm{Re}(p)>0$, and the two properties

$$\Gamma(p+1)=p\Gamma(p)\quad\text{and}\quad\Gamma(1-p)\Gamma(p)=\frac{\pi}{\sin(\pi p)}. \tag{B 6}$$

The beta function is related to the gamma function by the equality

$$B(p,q)=\frac{\Gamma(p)\Gamma(q)}{\Gamma(p+q)}. \tag{B 7}$$

Let a be a real such that $0<a<1$, it is immediate to remark that

$$\int_0^x t^{-a}(1-t)^a\,\mathrm{d}t=B(x,1-a,1+a). \tag{B 8}$$

Indeed, it is sufficient to let $p=1-a$ and $q=1+a$ and recall (B 2).

Moreover,

$$\int_0^1 t^{-a}(1-t)^a\,\mathrm{d}t=B(1,1-a,1+a)=B(1-a,1+a),$$

where we used (B 3). On the other hand, by (B 7) and the fact that $\Gamma(2)=1$, we have that

$$B(1-a,1+a)=\Gamma(1-a)\Gamma(1+a)=\Gamma(1-a)a\Gamma(a),$$

where in the last step we have used the first of (B 6). Hence, recalling the second of (B 6), we have that

$$\int_0^1 t^{-a}(1-t)^a\,\mathrm{d}t=\frac{\pi a}{\sin(\pi a)}. \tag{B 9}$$

Finally, with simple algebra, we get that

$$\int_0^1\mathrm{d}x\int_0^x t^{-a}(1-t)^a\,\mathrm{d}t=B(1-a,1+a)-\int_0^1 B(x,1-a,1+a)\,\mathrm{d}x.$$

By (B 4), we find

$$\int_0^1\mathrm{d}x\int_0^x t^{-a}(1-t)^a\,\mathrm{d}t=B(2-a,1+1).$$

On the other hand, by using the properties of the gamma and the beta functions as above and recalling that $\Gamma(3)=2$, we have that

$$B(2-a,1+1)=\frac{\Gamma(2-a)\Gamma(1+a)}{\Gamma(3)}=\frac{\Gamma(2-a)\Gamma(1+a)}{2}=\frac{1}{2}(1-a)a\Gamma(1-a)\Gamma(a).$$

By the second of (B 6), we thus get

$$\int_0^1\mathrm{d}x\int_0^x t^{-a}(1-t)^a\,\mathrm{d}t=\frac{1}{2}(1-a)a\frac{\pi}{\sin(\pi a)}. \tag{B 10}$$

References

1. Bray AJ. 1994 Theory of phase-ordering kinetics. *Adv. Phys.* **43**, 357–459. (doi:10.1080/00018739400101505)
2. Langer JS. 1992 *Solids far from equilibrium* (ed. C Godrèche). Cambridge, UK: Cambridge University Press.
3. Eyre DJ. 1993 Systems of Cahn–Hilliard equations. *SIAM J. Appl. Math.* **53**, 1686–1712. (doi:10.1137/0153078)
4. Fife PC. 2002 Pattern formation in gradient systems. *Handbook of dynamical systems* (ed. B Fielder), vol. 2, pp. 677–722. Amsterdam, The Netherlands: Elsevier Science.
5. Alikakos N, Bates PW, Fusco G. 1991 Slow motion for the Cahn–Hilliard equation in one space dimension. *J. Differ. Equ.* **90**, 81–135. (doi:10.1016/0022-0396(91)90163-4)
6. Allen SM, Cahn JW. 1979 A microscopic theory for antiphase boundary motion and its application to antiphase domain coarsening. *Acta Metall.* **27**, 1085–1095. (doi:10.1016/0001-6160(79)90196-2)
7. Gurtin ME. 1996 Generalized Ginzburg-Landau and Cahn-Hilliard equations based on a microforce balance. *Phys. D* **92**, 178–192. (doi:10.1016/0167-2789(95)00173-5)
8. Podio-Guidugli P. 2006 Models of phase segregation and diffusion of atomic species on a lattice. *Ric. Mat.* **55**, 105–118. (doi:10.1007/s11587-006-0008-8)
9. Benzi R, Sbragaglia M, Bernaschi M, Succi S. 2011 Phase-field model of long-time glasslike relaxation in binary fluid mixtures. *Phys. Rev. Lett.* **106**, 164501. (doi:10.1103/PhysRevLett.106.164501)
10. Cueto–Felgueroso L, Juanes R. 2012 Macroscopic phase-field model of partial wetting: bubbles in a capillary tube. *Phys. Rev. Lett.* **108**, 144502. (doi:10.1103/PhysRevLett.108.144502)
11. Alikakos N, Fusco G. 2008 On the connection problem for potentials with several global minima. *Indiana Univ. Math. J.* **57**, 1871–1906. (doi:10.1512/iumj.2008.57.3181)
12. Witelski TP. 1998 Equilibrium interface solutions of a degenerate singular Cahn-Hilliard equation. *Appl. Math. Lett.* **11**, 127–133. (doi:10.1016/S0893-9659(98)00092-5)
13. Rosenau P, Hyman JM. 1993 Compactons: solitons with finite wavelength. *Phys. Rev. Lett.* **70**, 564. (doi:10.1103/PhysRevLett.70.564)
14. Bertini L, Brassesco S, Buttà P. 2008 Soft and hard wall in a stochastic reaction diffusion equation. *Arch. Rational Mech. Anal.* **190**, 307–345. (doi:10.1007/s00205-008-0154-0)
15. Fusco G, Hale J. 1989 Slow-motion manifolds, dormant instability and singular perturbations. *J. Dyn. Differ. Equ.* **1**, 75–94. (doi:10.1007/BF01048791)
16. Chafee N, Infante EF. 1974 A bifurcation problem for a nonlinear partial differential equation of parabolic type. *Appl. Anal.* **4**, 17–37. (doi:10.1080/00036817408839081)
17. Cirillo ENM, Ianiro N, Sciarra G. 2010 Phase coexistence in consolidating porous media. *Phys. Rev. E* **81**, 061121–1–9. (doi:10.1103/PhysRevE.81.061121)
18. Cirillo ENM, Ianiro N, Sciarra G. 2012 Kink localization under asymmetric double-well potentials. *Phys. Rev. E* **86**, 041111. (doi:10.1103/PhysRevE.86.041111)
19. Cirillo ENM, Ianiro N, Sciarra G. 2013 Allen–Cahn and Cahn–Hilliard-like equations for dissipative dynamics of saturated porous media. *J. Mech. Phys. Solids* **61**, 1080–1114. (doi:10.1016/j.jmps.2012.08.014)
20. Cahn JW, Hilliard JE. 1958 Free energy of a nonuniform system. I. Interfacial free energy. *J. Chem. Phys.* **28**, 258–267. (doi:10.1063/1.1744102)
21. de Gennes PG. 1985 Wetting: statics and dynamics. *Rev. Modern Phys.* **57**, 827–863. (doi:10.1103/RevModPhys.57.827)